

Article

Mononuclear Tricoordinate Copper(I) and Silver(I) Halide Complexes of a Sterically Bulky Thiourea Ligand and a Computational Insight of Their Interaction with Human Insulin

 Awal Noor ^{1,*} , Sadaf Qayyum ¹, Farukh Jabeen ² and Ashfaq Ur Rehman ³
¹ Department of Basic Sciences, Preparatory Year Deanship, King Faisal University, Al-Hassa 31982, Saudi Arabia; sqayyum@kfu.edu.sa

² Department of Chemistry and Biochemistry, Laurentian University, 935 Ramsey Lake Road, Sudbury, ON P3E 2C6, Canada; fjabeen@laurentian.ca

³ Department of Molecular Biology and Biochemistry, University of California, Irvine, CA 92697-3900, USA; aurehman@uci.edu

* Correspondence: anoor@kfu.edu.sa

Abstract: Reaction of two equivalents of the bulky 1,3-bis(2,6-diethylphenyl)thiourea ligand (L) with MX (being M = Cu⁺, Ag⁺; and X = Cl⁻, Br⁻, I⁻) in acetonitrile afforded neutral complexes of the type [MXL₂] [CuCIL₂].2CH₃CN (**1a**); [CuBrL₂].2CH₃CN (**1b**); [CuIL₂] (**1c**); [AgCIL₂] (**2a**); [AgBrL₂] (**2b**) and [AgIL₂] (**2c**). The two aromatic groups in free ligand were found to be *trans* with respect to the thiourea unit, which was a reason to link the ligand molecules via intermolecular hydrogen bonding. Intramolecular hydrogen bonding was observed in all metal complexes. The copper complexes **1a** and **1b** are acetonitrile solvated and show not only intra- but also intermolecular hydrogen bonding between the coordinated thiourea and the solvated acetonitrile molecules. Silver complexes reported here are the first examples of structurally characterized tricoordinated thiourea-stabilized monomeric silver(I) halides. Molecular docking studies were carried out to analyze the binding modes of the metal complexes inside the active site of the human insulin (HI) protein. Analysis of the docked conformations revealed that the electrostatic and aromatic interactions of the protein *N*-terminal residues (i.e., Phe and His) may assist in anchoring and stabilizing the metal complexes inside the active site. According to the results of docking studies, the silver complexes exhibited the strongest inhibitory capability against the HI protein, which possesses a deactivating group, directly bonded to silver. All compounds were fully characterized by elemental analysis, NMR spectroscopy, and molecular structures of the ligand, and five out of six metal complexes were also confirmed by single-crystal X-ray diffraction.

Keywords: copper; coordination chemistry; human insulin; metal complexes; molecular docking; silver; S-ligands; thiourea; X-ray structures



Citation: Noor, A.; Qayyum, S.; Jabeen, F.; Rehman, A.U. Mononuclear Tricoordinate Copper(I) and Silver(I) Halide Complexes of a Sterically Bulky Thiourea Ligand and a Computational Insight of Their Interaction with Human Insulin. *Molecules* **2022**, *27*, 4231. <https://doi.org/10.3390/molecules27134231>

Academic Editor: Alberto Pettignano

Received: 3 June 2022

Accepted: 28 June 2022

Published: 30 June 2022

Publisher's Note: MDPI stays neutral with regard to jurisdictional claims in published maps and institutional affiliations.



Copyright: © 2022 by the authors. Licensee MDPI, Basel, Switzerland. This article is an open access article distributed under the terms and conditions of the Creative Commons Attribution (CC BY) license (<https://creativecommons.org/licenses/by/4.0/>).

1. Introduction

Thiourea ligands are of interest mainly due to their ready accessibility and broad applications in catalysis, biological activity, and optical technology [1–4]. The presence of soft sulfur and harder nitrogen donor atoms makes these ligands show different bonding possibilities and thus exhibit versatility in coordination chemistry. Thioureas can act as neutral, monoanionic, or dianionic ligands [5–7]. Despite the fact that it is a mature field of research, it nevertheless continues to attract the attention of synthetic chemists due to the possible variation of steric and electronic effects at the nitrogen atoms. This, in turn, alters their physical as well as chemical properties and has thus led to the isolation of not only efficient but also air- and moisture-stable catalysts, for instance for azide-alkyne addition and Heck reactions [8–10]. One of the focuses in the past has been the synthesis of

N-alkyl/aryl- and *N,N'*-dialkyl/diaryl-substituted thioureas and their coordination chemistry [11–17]. Among structurally characterized tricoordinate univalent metals, copper has been extensively studied, and silver rarely studied [18–20]. In particular, anhydrous metal (I) halide complexes of symmetrical *N,N'*-diaryl-substituted thioureas are rare, and among them, the structurally characterized tricoordinate silver (I) halides of thiourea are unknown [8]. Thus, we were interested in synthesizing and structurally characterizing *N,N'*-diaryl-substituted thiourea metal complexes of univalent copper and silver. First reported in 1997, 1,3-bis(2,6-diethylphenyl)thiourea is a symmetrically substituted ligand [21]. Surprisingly, to the best of our knowledge, metal complexes of it have not been reported to date. In addition to their structural importance, thiourea derivatives are also known for their diverse biological applications. The thiourea complexes of Cu and Ag have received special attention in bioinorganic applications mainly due to their low toxicity and their binding ability to human proteins [22–24]. The ability of thiourea to form hydrogen bonds favorably affects the solubility of its complexes in an aqueous medium, which contributes to better penetration into cells [25]. In this context, biological applications of coordination compounds are of particular importance to us [26–29]. Thiourea derivatives and their transition metal complexes have been shown to be quite potent antidiabetic agents [30–32].

Molecular docking has emerged as one of the most efficient virtual screening methods. It offers the possibility to predict the binding affinity between the applied compound and the target protein, but it also provides a helpful insight into the structure of the protein–target complex. The approach has been the focus of recent research activities for the discovery of a great number of new drugs, despite the fact that it is still far from full success in terms of its success rate. The promising antidiabetic behavior of free thioureas and our recent contribution prompted us to investigate the potential of these thiourea complexes with the human insulin receptor sites using molecular docking studies [33]. Herein, we report the synthesis and detailed characterization of thiourea ligands stabilized with univalent copper and silver complexes and provide a theoretical insight into their interaction with human insulin.

2. Experimental Section

2.1. Materials and Methods

Analytical grade solvents were used without any further purification. Deuterated solvents were obtained from Cambridge Isotope Laboratories and were degassed and dried prior to use. Thiourea ligand (1,3-bis(2,6-diethylphenyl)thiourea = **L**) was obtained from the reaction of CS₂ with a solution of 2,6-diethylaniline, trimethylamine, and water. Although the used ligand has been previously reported [21], we instead followed the synthetic methodology adopted by Cowley and co-workers [34]. NMR spectra were recorded on a Varian spectrometer at 300 MHz and 400 MHz at ambient temperature. The chemical shifts are reported in ppm relative to the internal TMS. Elemental analyses (CHN) were determined using a Vario EL III instrument. X-ray crystal structure analyses were performed by using a STOE-IPDS II and a STOE STADIVARI ($\lambda(\text{Mo-K}\alpha) = 0.71073 \text{ \AA}$) diffractometers equipped with Oxford Cryostream low-temperature units. Structure solution and refinement was accomplished using SIR97 [35], SHELXL2014 [36], WinGX [37], and Olex2 [38]. For **L** and **2c**, we observed one B-alert each in the checkcif files due to the missing of low-angle reflections as a result of beam stop and bad crystal quality, respectively. Selected crystallographic data are gathered in Table 1.

Table 1. Crystallographic data for **L**, **1a**, **1b**, **1c**, **2a**, and **2c**.

Compound	L	1a	1b	1c	2a	2c
Empirical formula	C ₂₁ H ₂₈ N ₂ S	C ₄₆ H ₆₂ ClCuN ₆ S ₂	C ₄₆ H ₆₂ BrCuN ₆ S ₂	C ₄₂ H ₅₆ CuIN ₄ S ₂	C ₄₂ H ₅₆ AgClN ₄ S ₂	C ₄₂ H ₅₆ AgIN ₄ S ₂
Formula weight	340.51	862.176	906.58	871.46	824.34	915.79
Crystal system	monoclinic	monoclinic	monoclinic	Triclinic	Orthorhombic	Orthorhombic
Space group	P2 ₁ /c1	P2 ₁ /n	P2 ₁ /n	P-1	P b c a	P b c a
a (Å)	18.370(4)	8.1700(16)	8.1490(6)	13.0940(6)	18.532(4)	18.8900(6)
b (Å)	27.610(6)	31.440(6)	31.597(2)	15.2930(7)	15.377(3)	15.5390(4)
c (Å)	23.010(5)	17.850(4)	17.9060(12)	22.5210(11)	28.753(6)	28.7440(8)
α (deg)				80.430(4)		
β (deg)	93.30(3)	90.50(3)	90.282(5)	80.507(4)		
γ (deg)				72.124(4)		
V (Å ³)	11,651(4)	4584.9(16)	4610.5(6)	4201.0(4)	8193(3)	8437.3(4)
Crystal size (mm ³)	0.80 × 0.71 × 0.51	0.21 × 0.08 × 0.06	0.77 × 0.56 × 0.25	0.25 × 0.18 × 0.14	0.26 × 0.24 × 0.15	0.16 × 0.12 × 0.08
ρ _{calcd} (g cm ⁻³)	1.165	1.249	1.306	1.378	1.337	1.442
μ (mm ⁻¹) (Mo Kα)	0.171	0.664	1.469	1.387	0.693	1.342
T (K)	133(2)	293(2)	133(2)	133(2)	133(2)	133(2)
2θ range (deg)	4.33–59.07	4.56–55.13	2.57–53.28	2.82–51.17	2.20–53.37	3.67–57.39
No. of reflections unique	29,725	10,751	9242	16,774	8220	10,515
No. of reflections obs. (I > 2σ (I))	16,193	5400	7002	7906	4862	7605
No. of parameters	1321	523	531	949	459	475
wR ² (all data)	0.2338	0.0961	0.0995	0.1310	0.1043	0.1613
R value (I > 2σ (I))	0.0727	0.0480	0.0385	0.0487	0.0403	0.0561

2.2. Synthesis of Compounds **1a–c** and **2a–c**

For the synthesis of **1a**, acetonitrile (30 mL) was added to ligand (0.169 g, 0.5 mmol) and CuCl (0.025 g, 0.25 mmol) at room temperature. The resulting suspension was stirred overnight, resulting in a small amount of white precipitation. The precipitate was separated by filtration, and the filtrate was allowed to afford colorless crystals of **1a**. Both precipitate and the crystalline material were identified to be the same material of the desired compound **1a**. Following the same procedure, **1b** was prepared by treating ligand (0.169 g, 0.5 mmol) with CuBr (0.36 g, 0.25 mmol). For **1c**, ligand (0.169 g, 0.5 mmol) was treated with CuI (0.048 g, 0.25 mmol). Acetonitrile was evaporated and the crystalline material was re-dissolved in CHCl₃ and filtered. The filtrate was allowed to slowly evaporate to afford colorless crystals of **1c** at room temperature. Following the synthetic procedure of **1a**, compound **2a** was prepared by reacting ligand (0.169 g, 0.5 mmol) with AgCl (0.036 g, 0.25 mmol). For **2b**, ligand (0.228 g, 0.67 mmol) was reacted with AgBr (0.063 g, 0.33 mmol). Compound **2c** was prepared by reacting ligand (0.169 g, 0.5 mmol) with AgI (0.059 g, 0.25 mmol). Acetonitrile was evaporated, and the crystalline material was re-dissolved in CHCl₃ and filtered. Slow evaporation of solvent from filtrate at room temperature afforded colorless crystals of **2c**.

Complex 1a: Yield: 90% (0.175 g). EA: Calculated for C₄₂H₅₆CuClN₄S₂ (780.05): C 64.67, H 7.24, N 7.18; found: C 64.80, H 7.00, N 7.14. ¹H NMR (CDCl₃, 400 MHz): δ = 1.13 (t, 12H, H^{CH3(CH2)}, J = 7.4 Hz), 1.35 (t, 12H, H^{CH3(CH2)}, J = 7.4 Hz), 2.55–2.70 (m, 16H, H^{CH3(CH2)}), 2.92–3.00 (m, 4H, H^{CH3(CH2)}), 6.35 (s, 2H, H^{NH}), 7.09 (d, 8H, H^{C6H5}, J = 7.4 Hz), 7.23 (d, 8H, H^{C6H5}, J = 7.4 Hz), 7.34 (t, 4H, H^{C6H5}, J = 7.4 Hz), 10.52 (s, 2H, H^{NH}) ppm. ¹³C NMR (CDCl₃, 100 MHz): δ = 14.5 (C^{CH3(CH2)}), 14.7 (C^{CH3(CH2)}), 24.5 (C^{CH3(CH2)}), 24.8 (C^{CH3(CH2)}), 126.4 (C^{CH}), 127.0 (C^{CH}), 128.8 (C^{CH}), 129.6 (C^{CH}), 131.9 (C^C), 133.3 (C^C), 142.0 (C^C), 143.0 (C^C), 178.9 (C^{C=S}) ppm.

Complex 1b: Yield: 74% (0.210 g). EA: Calculated for C₄₂H₅₆CuBrN₄S₂ (824.50): C 61.18, H 6.85, N 6.90; found: C 61.22, H 7.10, N 6.99. ¹H NMR (CDCl₃, 300 MHz): δ = 1.14 (t, 12H, H^{CH3(CH2)}, J = 7.5 Hz), 1.38 (t, 12H, H^{CH3(CH2)}, J = 7.5 Hz), 2.58 (m, 8H, H^{CH3(CH2)}), 2.64 (q, 4H, H^{CH3(CH2)}), 2.98 (m, 4H, H^{CH3(CH2)}), 6.35 (s, 2H, H^{NH}), 7.07–7.40 (m, 12H, H^{C6H3}), 10.28 (s, 2H, H^{NH}) ppm. ¹³C NMR (CDCl₃, 75 MHz): δ = 14.4 (C^{CH3(CH2)}), 14.8 (C^{CH3(CH2)}), 24.4 (C^{CH3(CH2)}), 24.7 (C^{CH3(CH2)}), 126.2 (C^{CH}), 126.9 (C^{CH}), 128.7 (C^{CH}), 129.7 (C^{CH}), 131.7 (C^C), 133.1 (C^C), 141.9 (C^C), 143.0 (C^C), 178.6 (C^{C=S}) ppm.

Complex 1c: Yield: 93% (0.200 g). EA: Calculated for C₄₂H₅₆CuIN₄S₂ (871.50): C 57.88, H 6.48, N 6.43; found: C 57.59, H 6.38, N 6.37. ¹H NMR (CDCl₃, 300 MHz): δ = 1.13 (t, 12H, H^{CH3(CH2)}, J = 7.5 Hz), 1.38 (t, 12H, H^{CH3(CH2)}, J = 7.5 Hz), 2.58 (q, 8H, H^{CH3(CH2)}, J = 7.5 Hz), 2.70 (q, 4H, H^{CH3(CH2)}, J = 7.5 Hz), 2.97 (q, 4H, H^{CH3(CH2)}, J = 7.5 Hz),

6.37 (s, 2H, H^{NH}), 7.06–7.40 (m, 12H, H^{C6H3}), 9.98 (s, 2H, H^{NH}) ppm. ¹³C NMR (CDCl₃, 75 MHz): δ = 14.3 (C^{CH3(CH2)}), 15.0 (C^{CH3(CH2)}), 24.3 (C^{CH3(CH2)}), 24.3 (C^{CH3(CH2)}), 126.1 (C^{CH}), 126.9 (C^{CH}), 128.6 (C^{CH}), 129.7 (C^{CH}), 131.3 (C^C), 132.9 (C^C), 141.8 (C^C), 143.0 (C^C), 178.0 (C^{C=S}) ppm.

Complex 2a: Yield: 91% (0.188 g). EA: Calculated for C₄₂H₅₆AgClN₄S₂ (824.37): C 61.19, H 6.85, N 6.80; found: C 60.57, H 6.90, N 6.70. ¹H NMR (CDCl₃, 300 MHz): δ = 1.17 (t, 12H, H^{CH3(CH2)}, J = 7.75 Hz), 1.38 (t, 12H, H^{CH3(CH2)}, J = 7.75 Hz), 2.57 (q, 8H, H^{CH3(CH2)}, J = 7.75 Hz), 2.68–2.76 (m, 4H, H^{CH3(CH2)}), 2.94–3.06 (m, 4H, H^{CH3(CH2)}), 6.45 (s, 2H, H^{NH}), 7.12 (d, 8H, H^{C6H5}, J = 7.2 Hz), 7.25 (d, 8H, H^{C6H5}, J = 7.75 Hz), 7.31–7.34 (m, 4H, H^{C6H5}), 10.86 (s, 2H, H^{NH}) ppm. ¹³C NMR (CDCl₃, 75 MHz): δ = 14.4 (C^{CH3(CH2)}), 14.5 (C^{CH3(CH2)}), 24.4 (C^{CH3(CH2)}), 24.7 (C^{CH3(CH2)}), 126.3 (C^{CH}), 126.8 (C^{CH}), 128.7 (C^{CH}), 129.6 (C^{CH}), 131.7 (C^C), 133.4 (C^C), 142.0 (C^C), 142.9 (C^C), 178.7 (C^{C=S}) ppm.

Complex 2b: Yield: 92% (0.267 g). EA: Calculated for C₄₂H₅₆AgBrN₄S₂ (868.82): C 58.06, H 6.50, N 6.45; found: C 57.76, H 6.19, N 6.48. ¹H NMR (CDCl₃, 400 MHz): δ = 1.14 (t, 12H, H^{CH3(CH2)}, J = 7.5 Hz), 1.36 (t, 12H, H^{CH3(CH2)}, J = 7.5 Hz), 2.55–2.72 (m, 16H, H^{CH3(CH2)}), 2.92–3.01 (m, 4H, H^{CH3(CH2)}), 6.43 (s, 2H, H^{NH}), 7.11 (d, 8H, H^{C6H5}, J = 7.5 Hz), 7.25 (d, 8H, H^{C6H5}, J = 7.5 Hz), 7.35 (t, 4H, H^{C6H5}, J = 7.5 Hz), 10.0 (s, 2H, H^{NH}) ppm. ¹³C NMR (CDCl₃, 100 MHz): δ = 14.5 (C^{CH3(CH2)}), 14.7 (C^{CH3(CH2)}), 24.5 (C^{CH3(CH2)}), 24.9 (C^{CH3(CH2)}), 126.5 (C^{CH}), 127.0 (C^{CH}), 128.9 (C^{CH}), 129.8 (C^{CH}), 131.7 (C^C), 133.5 (C^C), 142.1 (C^C), 143.1 (C^C), 179.1 (C^{C=S}) ppm.

Complex 2c: Yield: 94% (0.214 g). EA: Calculated for C₄₂H₅₆AgIN₄S₂ (915.83): C 55.08, H 6.16, and N 6.12; found: C 55.04, H 5.85, and N 6.19. ¹H NMR (CDCl₃, 300 MHz): δ = 1.14 (t, 12H, H^{CH3(CH2)}, J = 7.5 Hz), 1.35 (t, 12H, H^{CH3(CH2)}, J = 7.5 Hz), 2.60 (q, 8H, H^{CH3(CH2)}, J = 7.5 Hz), 2.69 (m, 4H, H^{CH3(CH2)}), 2.99 (m, 4H, H^{CH3(CH2)}), 6.43 (s, 2H, H^{NH}), 7.08–7.37 (m, 12H, H^{C6H3}), 9.31 (s, 2H, H^{NH}) ppm. ¹³C NMR (CDCl₃, 75 MHz): δ = 14.4 (C^{CH3(CH2)}), 14.9 (C^{CH3(CH2)}), 24.4 (C^{CH3(CH2)}), 24.7 (C^{CH3(CH2)}), 126.2 (C^{CH}), 126.9 (C^{CH}), 128.5 (C^{CH}), 129.7 (C^{CH}), 131.5 (C^C), 133.6 (C^C), 141.9 (C^C), 143.2 (C^C), 179.7 (C^{C=S}) ppm.

2.3. Molecular Docking

The synthesized metal-based ligand complexes were studied using a molecular docking simulation with the crystal structure of human insulin (HI) as a target protein. The HI was retrieved from the RCSB protein data bank (<https://www.rcsb.org/> accessed on 27 February 2022). The co-crystallized macromolecule cucurbit [7] uril is included in the HI protein structure. In order to elucidate the molecular mechanism of inhibition, the metal complexes (**1a–c** and **2a–c**) were docked in the active sites of the HI protein using the molecular operating environment (MOE) v2020 tool [39] and PDB code 3Q6E [40]. The target was prepared using the protein preparing module of the MOE. All solvent molecules were removed before the docking studies could begin. The cleft-like active site was mapped around the cognate ligand. Highly stiff complexes were found to benefit from the HI protein's availability of a cleft-like pocket. As an active site, we leveraged that cleft. Finally, refined crystal structure was used for further docking study using the default parameters of MOE (i.e., Placement: Triangle Matcher, Rescoring 1: London dG, Refinement: Force-field, Rescoring 2: GBVI/WSA). For the ligand, a total of 50 conformations were chosen before executing the docking approach. For the protein–ligand interaction (PLI) study, the top-ranked conformations by docking score and binding energy were chosen. Additionally, we have evaluated the specificity of the target with the metal complex using dynamut and WEBnm [41,42].

3. Results and Discussion

Structures of substituted thioureas have always been of interest mainly due to the difficulty in obtaining crystals suitable for X-ray analysis [43–56]. Crystals of ligand **L** partially suitable for X-ray analysis were grown from its chloroform solution by slow evaporation.

Compound **L** crystallized in monoclinic crystal system in P2₁/c space group with six molecules in the unit cell. The two aromatic groups are in *trans* position with respect

to the thiourea unit (Figure 1). This configuration favors dimer formation between the molecules, and in this case, intermolecular N–H···S hydrogen bonds (3.266 and 3.328 Å) link the molecules into dimers (Figure 2). One of the ethyl groups shows disorder, and this is the reason for the relatively large displacement parameter and an unusual C8–C9 bond distance (1.428(6) Å). The short C–S distance (1.682(3) Å) clearly shows its double bond character (for comparison, C–S single bond is 1.82 Å) [57]. The S1–C1–N1–C2 and N2–C1–N1–C2 torsion angles are 1.58 and 178.42°, respectively. Experimental details of the X-ray single crystal structure analyses are summarized in Table 1.

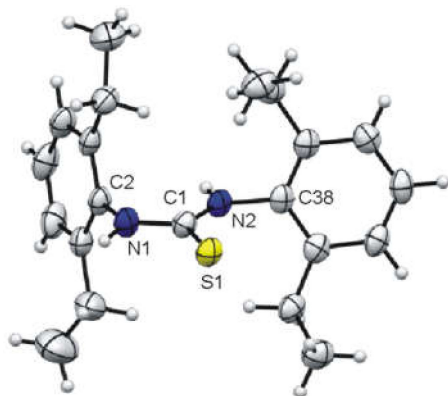


Figure 1. Molecular structure of 1,3-bis(2,6-diethylphenyl)thiourea ligand (ellipsoids correspond to the 50% probability level). Selected bond lengths (Å) and angles (°): S1–C1 1.682(3), N2–C1 1.342(3), N2–C38 1.437(4), C1–N1 1.350(4), C2–N1 1.432(3); C1–N2–C38 126.5(2), N2–C1–N1 116.2(2), N2–C1–S1 123.1(2), N1–C1–S1 120.7(2), C1–N1–C2 126.5(2).

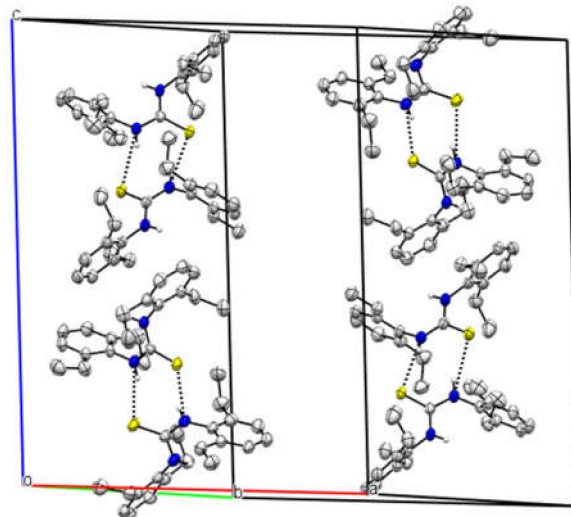
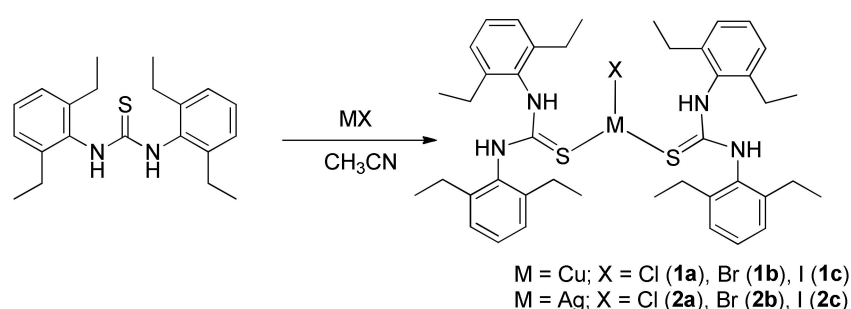


Figure 2. The partial packing figure of 1,3-bis(2,6-diethylphenyl)thiourea ligand along a, b and c axes (which shows the intermolecular H-bonds). Only N–H hydrogens are shown. Color scheme: S = yellow; N = blue; C = grey; and H = white.

To isolate the metal complexes, acetonitrile was added to **L** and the corresponding metal (I) halide (metal = Cu, Ag; halide = Cl, Br, I) in 2:1 ratio at room temperature (Scheme 1). The reaction mixture was then stirred overnight at room temperature. After filtration, the filtrate was concentrated and stored at room temperature to afford the corresponding crystalline compounds [MXL₂] [CuClL₂].2CH₃CN (**1a**); [CuBrL₂].2CH₃CN (**1b**); [CuIL₂] (**1c**); [AgClL₂] (**2a**); [AgBrL₂] (**2b**); and [AgIL₂] (**2c**) in high yields (74–94%). All the complexes were soluble in most common organic solvents, such as acetonitrile, acetone, methanol, methylene chloride, chloroform, and aqueous ethanol.



Scheme 1. Syntheses of mononuclear tricoordinated copper (I) and silver (I) complexes of bulky 1,3-bis(2,6-diethylphenyl)thiourea ligand.

The ^1H NMR spectra of **1** and **2** in CDCl_3 exhibit resonances for N–H protons at higher and lower fields ($\delta = 6.35$ and 10.52 ppm (**1a**), $\delta = 6.35$ and 10.28 ppm (**1b**), and $\delta = 6.37$ and 9.98 ppm (**1c**) and $\delta = 6.45$; and 10.86 ppm (**2a**), $\delta = 6.43$ and 10.0 ppm (**2b**), and $\delta = 6.43$ and 9.31 ppm (**2c**), respectively). The shift to lower field could be attributed to the possible presence of intramolecular hydrogen bonding between thiourea and halide ligands [58,59]. For comparison, a singlet appears at 6.42 ppm in CDCl_3 for the two N–H protons of the free ligand [21]. The ^{13}C NMR spectra of **1** and **2** show characteristic peaks at 178.9 ppm (**1a**), 178.6 ppm (**1b**), and 178.0 ppm (**1c**); and 178.7 ppm (**2a**), 179.1 ppm (**2b**), and 179.7 ppm (**2c**), respectively, for C=S moiety (see Supplementary Materials). The other aliphatic and aromatic chemical shifts for both bulky thiourea ligands are in the typical regions with very less variation. The NMR data of **1a/b** show that these complexes are stable even if the co-crystallized acetonitrile molecules are removed by drying the samples in high vacuum.

All complexes except **2b** were further characterized by X-ray structural and elemental analyses. All compounds are mononuclear three-coordinated metal(I) halide complexes, in which metal is coordinated by two sulfur atoms of each bulky thiourea ligand, and one halogen atom, thus exhibiting trigonal planar molecular configurations with a butterfly structure. The driving force for this structure might be the intramolecular hydrogen bonds between halogen and the two nitrogen atoms of the two ligands to form pseudo-six-membered rings (NHCuSC). Intermolecular hydrogen bonds observed were as a result of the solvated molecules. Experimental details of the X-ray single-crystal structure analyses are summarized in Table 1.

Compounds **1a** and **1b** both crystallize in a monoclinic crystal system with two CH_3CN molecules each in the unit cells. Solvent-free copper complex **1c** crystallizes (from CHCl_3) in triclinic space group P-1 with two molecules in the unit cell. In **1b**, one of the methyl of ethyl groups has relatively large displacement parameter due to disorder and is the reason for an unusual C21–C29 bond distance ($1.386(7)$ Å). In all three copper compounds, the two intramolecular N–H \cdots X (X = Cl, Br, I) hydrogen bonds complete the twisted six-membered rings (Figures 3–5). In **1a**, the two intramolecular hydrogen bonds N1–H1 \cdots Cl1 (3.349 Å) and N4–H4 \cdots Cl1 (3.367 Å) are nearly identical but longer than those observed for similar 1,3-bis(2,6-dimethylphenyl)thiourea Cu(I) chloride complex [3]. In **1b** and **1c**, one of the two hydrogen bond's D \cdots A distance (Å) and D–H \cdots A angle ($^\circ$), N1–H1N \cdots Br1 (3.464 , 177) and N3–H3N \cdots I1 (3.651 , 175), are longer and wider than the other, N3–H3N \cdots Br1 (3.393 , 169) and N1–H1N \cdots I1 (3.555 , 163). The bond angles observed for **1b** are identical to those reported by Tahir and co-workers for similar N,N' -bis(diphenyl)thiourea complexes (3.435 Å, 169° and 3.573 (2) Å, 170°) [60]. In **1a**, the Cu–Cl bond distance of $2.2440(9)$ Å is comprehensively shorter than the Cu–Cl bond distance ($2.3058(10)$ Å) recently published by Nembenna and co-workers [8]. The Cu–Br bond distance of $2.3721(4)$ Å in **1b** is slightly longer than the Cu–Br bond distance in N,N' -bis(diphenyl)thiourea stabilized copper(I) complex [20] but comparable to N,N' -dicyclohexylthiourea stabilized copper complex ($2.3801(5)$ Å) [61]. The slight increase in C=S bond distance of the bridging NCN moiety on binding with copper for **1a** and **1b** (average bond distance of 1.709 Å and 1.705 Å,

respectively) compared to free ligand is common for such ligands. The shorter Cu–I (2.5134(8) Å) and Cu1–S1 (2.2328(15) Å) and Cu1–S2 2.2197(15) Å) bond distances in **1c** than the previously known copper(I) iodide complexes could be attributed to the different coordination environment [62–64].

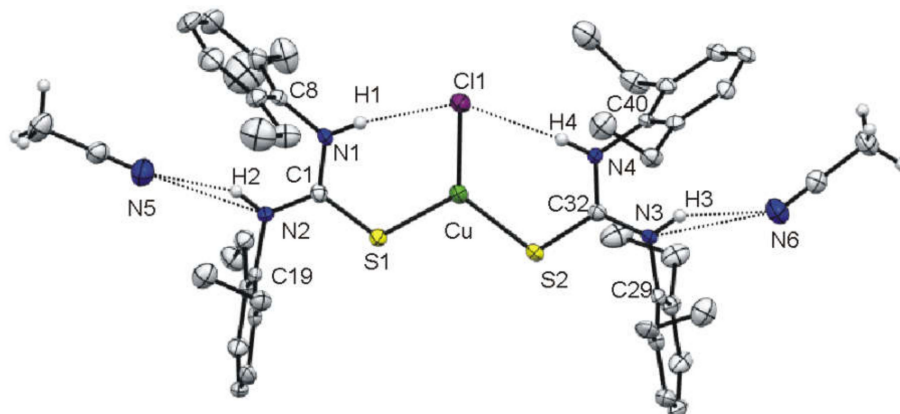


Figure 3. Molecular structure of **1a** (ellipsoids correspond to the 50% probability level). All hydrogen atoms, except those of N–H and CH₃ hydrogens of acetonitrile, have been deleted for clarity. Selected bond lengths (Å) and angles (°): Cu1–S1 2.2176(9), Cu1–Cl1 2.2440(9), Cu1–S2 2.2180(9), S1–C11 1.708(3), S2–C32 1.710(3), N3–C29 1.452(3), N3–C32 1.330(4), N2–C19 1.454(3), N2–C11 1.331(4), N4–C40 1.445(3), N4–C32 1.345(3), N1–C8 1.434(4), N1–C11 1.341(3); S1–Cu1–Cl1 123.36(3), S1–Cu1–S2 110.34(3), S2–Cu1–Cl1 126.29(3), C11–S1–Cu1 110.75(10), C32–S2–Cu1 108.85(10), C32–N3–C29 124.2(2), C11–N2–C19 122.1(2), C32–N4–C40 122.8(2), C11–N1–C08 125.2(3), C18–C19–N2 118.4(2), C14–C19–N2 118.7(3), N2–C11–S1 119.9(2), N2–C11–N1 118.7(3), N1–C11–S1 121.4(2), N3–C32–S2 121.1(2), N3–C32–N4 118.0(3), N4–C32–S2 120.9(2).

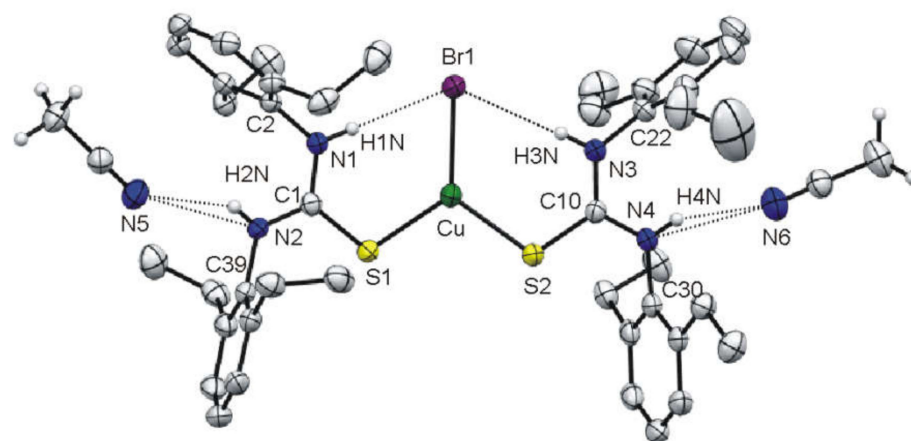


Figure 4. Molecular structure of **1b** (ellipsoids correspond to the 50% probability level). All hydrogen atoms, except those of N–H and CH₃ hydrogens of acetonitrile, have been deleted for clarity. Selected bond lengths (Å) and angles (°): Br1–Cu1 2.3721(4), Cu1–S1 2.2143(7), Cu1–S2 2.2186(7), S1–C1 1.707(2), S2–C10 1.703(2), N1–C1 1.331(3), N1–C2 1.441(3), N3–C10 1.331(3), N3–C22 1.441(3), C1–N2 1.336(3), N2–C39 1.431(3), N4–C10 1.338(3), N4–C30 1.438(3); S1–Cu1–S2 111.40(3), S1–Cu1–Br1 125.56(2), S2–Cu1–Br1 123.04(2), C1–S1–Cu1 109.82(8), C10–S2–Cu1 110.94(8), C1–N1–C2 123.8(2), C10–N3–C22 125.1(2), N1–C1–N2 117.8(2), N1–C1–S1 121.96(18), N2–C1–S1 120.19(18), C1–N2–C39 125.0(2), C10–N4–C30 122.8(2).

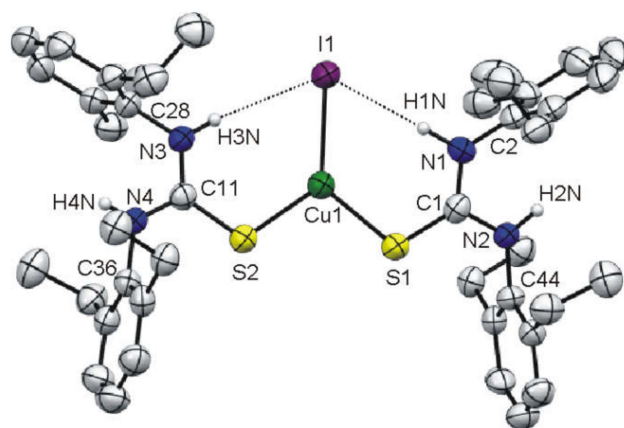


Figure 5. Molecular structure of **1c** (ellipsoids correspond to the 50% probability level). All hydrogen atoms, except those of N-H hydrogens and one molecule, have been deleted for clarity. Selected bond lengths (Å) and angles (°): I1–Cu1 2.5134(8), Cu1–S2 2.2197(15), Cu1–S1 2.2328(15), S1–C1 1.681(6), S2–C11 1.695(5), N2–C1 1.351(7), N2–C44 1.444(6), N3–C11 1.338(7), N3–C28 1.450(7), N1–C1 1.345(7), N1–C2 1.432(7), N4–C11 1.324(7), N4–C36 1.447(7); S2–Cu1–S1 108.03(6), S2–Cu1–I1 126.39(5), S1–Cu1–I1 125.57(5), C1–S1–Cu1 110.19(19), C11–S2–Cu1 111.91(18), C1–N2–C44 123.8(5), C11–N3–C28 122.9(5), C1–N1–C2 124.3(5), C11–N4–C36 125.1(5), N1–C1–N2 115.7(5), N1–C1–S1 123.2(4), N2–C1–S1 121.1(4), N4–C11–N3 117.4(5), N4–C11–S2 119.7(4), N3–C11–S2 122.9(4).

In **1a** and **1b**, the NH-groups not involved in H-bonding with halide-atom make intermolecular H-bonds with N-atoms of acetonitrile (N–H···N distances of 2.982 and 2.993 Å in **1a** and 2.988 and 2.980 Å in **1b**). It is interesting to see that two of the CH₃-hydrogens of the acetonitrile are also involved in hydrogen bonding (one with S-atom of thiourea (C–H···S 3.664 Å in **1a** and 3.670 Å in **1b**) and the other with N-atom (C–H···N 3.517 Å in **1a** and 3.543 Å in **1b**) of another acetonitrile), and the third makes a π interaction (only **1b** is shown in Figure 6).

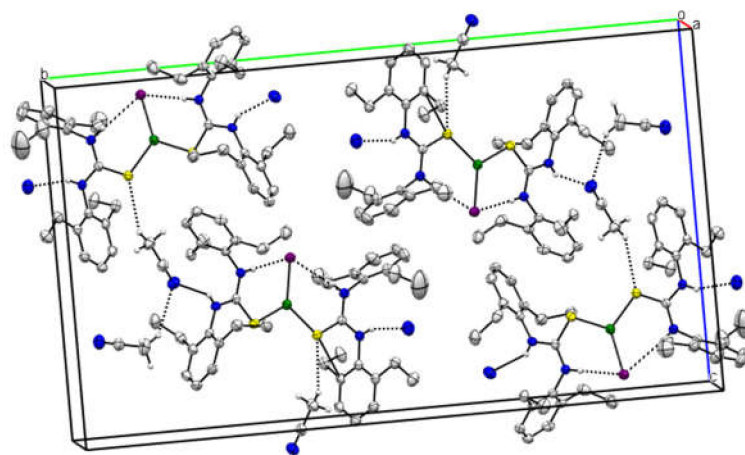


Figure 6. Perspective drawing of the packing arrangement of **1b** in the crystal along a, b and c axes. Only N–H and CH₃ hydrogens of acetonitrile are shown. Color scheme: Cu = green; S = yellow; N = blue; Br = purple; C = grey; and H = white.

Similar to **1a** and **1b**, crystals of silver complex **2a** were also obtained from acetonitrile, but without solvated molecules, whereas crystals of **2c** were grown from chloroform. Both **2a/c** crystallize in a orthorhombic crystal system in *Pbca* space group and are the first examples of structurally characterized tricoordinated thiourea-stabilized monomeric silver halide complexes (Figures 7 and 8) [65,66]. The longer intramolecular hydrogen bonds D···A distances in **2c** (N1–H1N···I1 3.543 Å and N3–H3N···I1 3.702 Å) compared to **2a** (N2–H2N···C11 3.278 Å and N3–H3N···C11 3.472 Å) are attributed to the larger size of the

iodide ligand. Although there is some variation in the S–Ag–X pair of angles (S1–Ag1–Cl1 116.94(3)° and S2–Ag1–Cl1 116.23(3)°; S1–Ag1–I1 120.00(3)° and S2–Ag1–I1 114.82(3)°), the S–Ag–S angles are essentially identical (S2–Ag1–S1 126.79(3)° (2a) and S2–Ag1–S1 125.09(5)° (2c)). The Ag–S bond exhibits slight increase from chloride to iodide (Ag1–S1 2.4362(9) Å and Ag1–S2 2.4257(8) (2a) Å; Ag1–S1 2.4673(12) and Ag1–S2 2.4594(12) (2c) Å). The Ag–S bonds observed in 2a are comparable to closely related tricoordinate silver(I) chloro complex of imidazolidine-2-thiones (2.439(1) Å) [67]. The increase in Ag–X (Ag1–Cl1 2.5040(10) Å and Ag1–I1 2.7505(6) Å) is attributed to the increased size of iodide ligand.

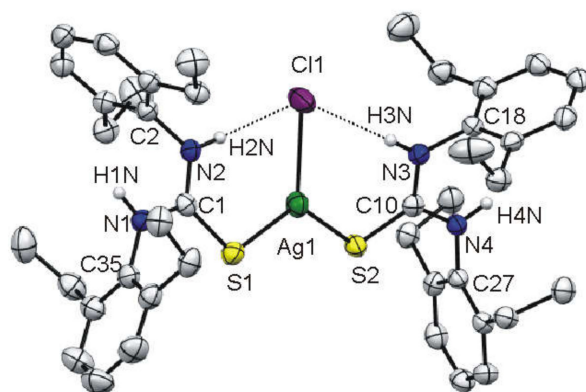


Figure 7. Molecular structure of 2a (ellipsoids correspond to the 50% probability level). Hydrogen atoms, except those of N–H, have been deleted for clarity. Selected bond lengths (Å) and angles (°): Ag1–S2 2.4257(8), Ag1–S1 2.4362(9), Ag1–Cl1 2.5040(10), S2–C10 1.690(3), S1–C1 1.698(3); S2–Ag1–S1 126.79(3), S2–Ag1–Cl1 116.23(3), S1–Ag1–Cl1 116.94(3), C10–S2–Ag1 108.36(11), C1–S1–Ag1 106.02(11), C1–N1–C35 126.1(3), C10–N3–C18 120.7(3), C10–N4–C27 124.0(3), C1–N2–C2 122.4(3), N2–C1–N1 117.3(3), N2–C1–S1 122.8(2), N1–C1–S1 119.9(2), N4–C10–N3 116.4(3), N4–C10–S2 119.7(2), N3–C10–S2 123.9(2).

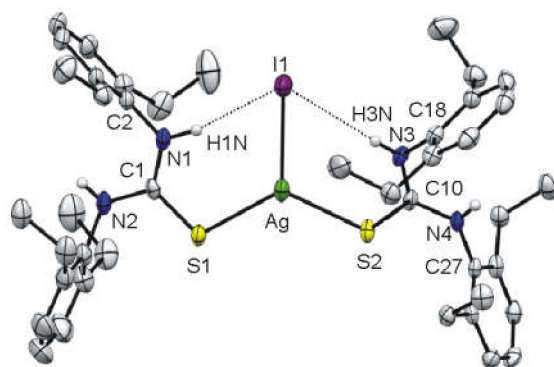


Figure 8. Molecular structure of 2c (ellipsoids correspond to the 50% probability level). Hydrogen atoms, except those of N–H, have been deleted for clarity. Selected bond lengths (Å) and angles (°): Ag1–S2 2.4594(12), Ag1–S1 2.4673(12), Ag1–I1 2.7505(6), S2–C10 1.705(5), S1–C1 1.710(5); S2–Ag1–S1 125.09(5), S2–Ag1–I1 114.82(3), S1–Ag1–I1 120.00(3), C10–S2–Ag1 110.48(16), C1–S1–Ag1 107.09(16), C10–N3–C18 121.5(4), C10–N4–C27 125.0(4), C1–N1–C2 123.7(4), N1–C1–N2 117.4(4), N1–C1–S1 122.8(3), N2–C1–S1 119.9(4), C1–N2–C35 127.0(4), N3–C10–N4 117.0(4), N3–C10–S2 123.9(3), N4–C10–S2 119.1(4).

The use of coordination compounds as metal-based drugs is known to lower the blood sugar levels in diabetic patients [68]. To develop a new drug, the fundamental quest is to understand their interaction and efficiencies with the receptor site. The availability of the 3D structure of the target protein makes molecular docking one of the best screen options. Molecular docking simulation was performed in order to evaluate the binding pattern of the synthesized metal complexes inside the active site of the human insulin (HI), using the default settings built in the MOE modelling tool.

In general, hydrophobic residues have been found to have a strong interaction with the ligand essential moiety. The best docking positions with the most interactions were those that were ranked first based on the least amount of energy (calculated as a negative value by MOE), as listed in Table 2. In order to further study the interactions of the metal-based docked conformations with the key residues, the most favorable docking poses of the 50 docked conformations for each metal complex were analyzed. Both the hydrophobic and hydrophilic portions were used to create the active site cleft (see in Figure 9a). Catalytic residues are mostly found in the hydrophilic region of the HI protein, and they may play an effective role in increasing or decreasing its activity.

Table 2. The interaction network for metal-based ligand complexes.

Compound	Ligand	Receptor	Interaction	Distance	E (kcal/mol)	Docking Score
1a	Cl	N PHE 1	H-acceptor	3.42	−10.7	−5.60408545
	S34	N PHE 1	H-acceptor	3.34	−4.5	
1b	S34	N PHE 1	H-acceptor	3.79	−4.9	−5.06169271
	6-ring	5-ring HIS 10	pi-pi	3.50	−0.0	
1c	C 6	NE2 GLN 4	H-acceptor	3.43	−0.5	−4.67316198
	6-ring	5-ring HIS 10	pi-pi	3.77	−0.0	
2a	Cl 5	NE2 GLN 4	H-acceptor	3.74	−1.6	−6.59288883
	S34	N PHE 1	H-acceptor	3.38	−5.8	
	6-ring	N PHE 1	pi-cation	3.33	−2.7	
2b	6-ring	5-ring HIS 10	pi-pi	3.75	−0.0	−5.93951702
	N 38	OE2 GLU 13	H-donor	3.16	−0.7	
2c	6-ring	5-ring HIS 10	pi-pi	3.45	−0.0	−5.07392883
	I 5	N PHE 1	H-acceptor	4.19	−7.1	
	6-ring	5-ring HIS 10	pi-pi	3.93	−0.0	

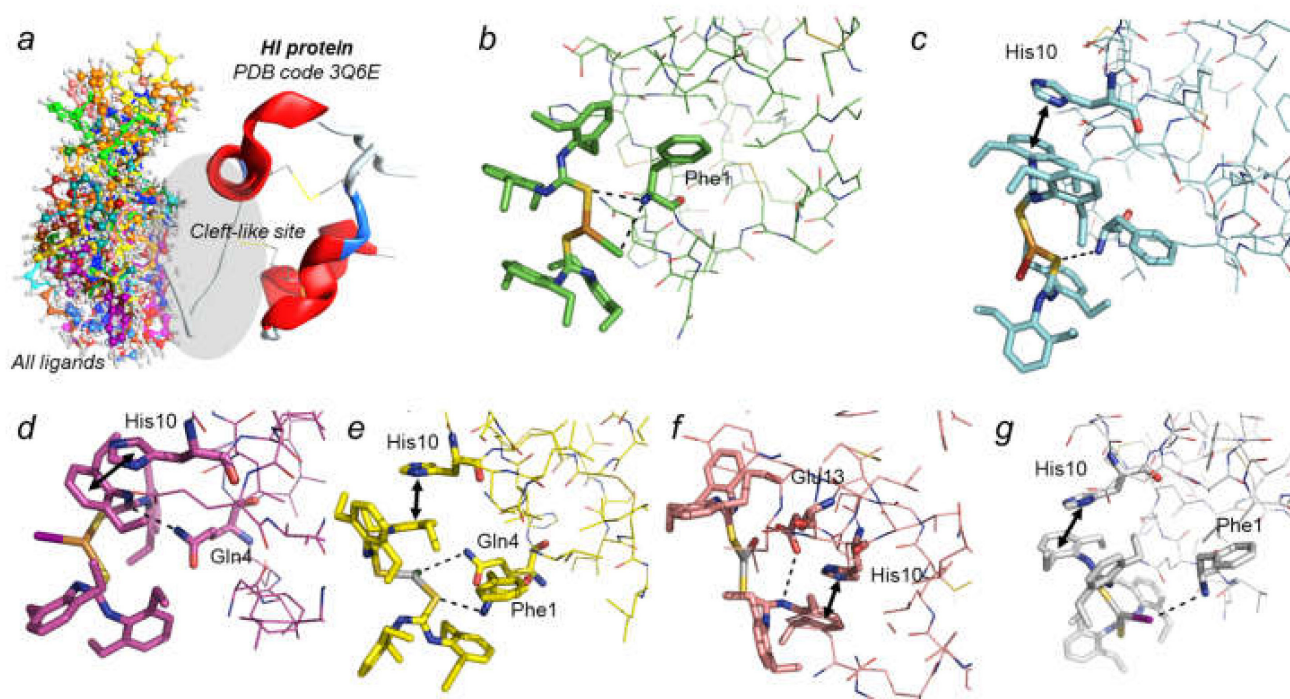


Figure 9. Analysis of the binding pattern of all the metal-based ligands complexes inside the active cleft of human insulin. (a) represents all the superposed docked metal-based ligands complexes; (b–g) represent the interaction profile for metal-based ligand complexes: (b) for 1a, (c) for 1b, (d) for 1c, (e) for 2a, (f) for 2b, and (g) for 2c. The molecule and interactive residues are shown as sticks, while the rest of the active site residues are shown in wireframe models. Hydrogen bonding interactions are shown as black dotted lines, metered with the distance in Å, and π - π interactions are shown by double-sided arrows.

Molecular docking studies showed that the metal complexes stabilize themselves inside the active site cleft through electrostatic and aromatic interactions. The N-terminal Phe and His residues may stabilize the molecules and prevent their dissociation from the active site residues. The hydrophobic and hydrophilic amino acid residues formed a stable host–guest complex by interacting via π -stacking and hydrogen bonding. The protein–ligand interaction profiles of the complexes are shown in Figure 9b–g. In all the complexes, the sulfur atom of the thiourea ligand was ligated with the corresponding metal atom of the complexes. Despite the rigid phenyl ring, all the complexes managed to attain the docking table conformation inside the active site cleft, as shown in Figure 9a. In addition to that, the phenyl established significant aromatic interactions with the active site residues, which played a significant role in anchoring the metal complexes inside the pocket of HI. The present docking study found that the silver-based complexes showed the strongest inhibitory potential against the HI protein, which possesses a deactivating group that is directly connected to silver. The deactivating group might withdraw some of the electronic density from the reaction center, leaving the moiety with a partial positive charge, which drives the moiety to form crucial contacts with critical residues, resulting in greater stability. Metal complexes **1a** and **2a**, containing chlorine, both exhibited interactions with the active site residue through the halogen atom, which can be attributed to the higher electronegative nature of chloride ion. Complexes having bromine and iodine did not show any type of electrostatic interactions with the active site residues. Thus, it can be argued that the electronegativity may play an important role in designing novel metal-based HI inhibitors. Since the halogen group withdraws electronic density from the compound, it needs to stabilize itself by adopting interaction with the active residues. In general, the hydrophobic residues preferred to establish the interactions with the important phenyl moiety of the complex. Aromatic moieties adopted interactions particularly with the sulfur and metal atoms, directly in the metal-based complexes. Interestingly, these hydrophobic residues bonded with high potential, and anchored the complex inside the active site of the protein with binding energy of around -10.7 to -7.1 kcal/mol, which is quite significant for stabilization of the metal complex inside the active site cavity. The impact of withdrawing the electronic density from the compound further compelled the compound to manage possible interaction for the ease of gaining a stable environment inside the active site cleft.

Additionally, we have evaluated the normal mode analysis (NMA) for **2a** in order to check the dynamic nature/equilibrium modes of the complex (Figure 10). The NMA can model amino acids using $C\alpha$ atoms to reduce computing cost. Normal mode analysis shows that the **2a** and protein complex is stabilized by harmonic potentials. The results indicate that upon binding with **2a**, the overall protein conformation remains compact and had a strong positive correlation instead of negative correlation, which further indicates that this complex remains in the active site and will need enough energy to be dissociated from the pocket. It was observed that the residues' fluctuation is much higher than that of the complex state, revealing the impact of the complex in the binding site, to rescue the protein from high conformation. Thus, it can be suggested that these complexes might be used as a stand-in surrogate for developing and designing novel drugs.

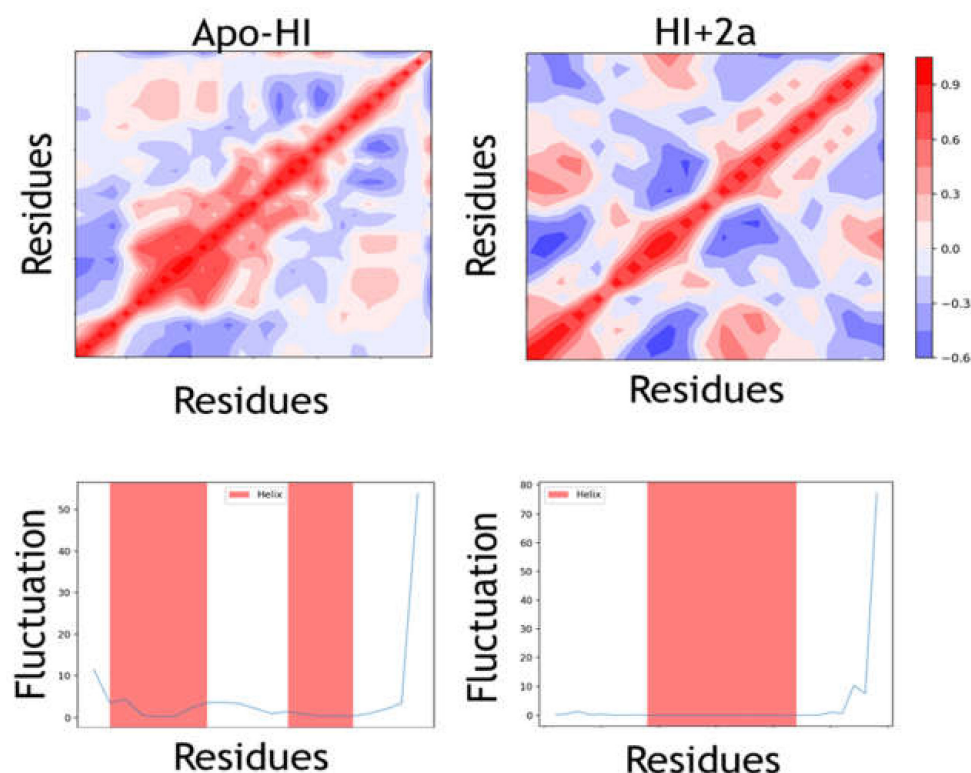


Figure 10. Normal mode analysis of **2a**. The upper panel (right with **2a** and left) indicates the correlation. The color bar indicates the positive (red) and negative (blue color) correlation. A stronger correlation indicates a more compact structure, while a negative correlation indicates a move-away behavior, which subsequently increases the plasticity of the structure, where it would be very easy for any compound to dissociate. The lower panel indicates the residue fluctuation.

4. Conclusions

The reaction of salts of univalent metals MX (where M = Cu or Ag and X = Cl, Br, and I) with sterically hindered thiourea ligand leads selectively to corresponding monomeric MXL₂ complexes. All compounds are neutral, and air and moisture stable. Intermolecular H-bonds were responsible for forming dimers in free ligand. The tricoordinate monomeric complexes of silver halides reported here are the first structurally characterized examples of the vastly studied thiourea ligands. Intramolecular H-bonds were observed between N–H ··· X atoms, whereas intermolecular H-bonds were evident between solvated acetonitrile and metal-coordinated thiourea ligands. The docking results demonstrated that the silver-based ligand complex **2a** has a strong inhibitory potential against the HI protein, which contains a deactivating group that is directly linked to silver. Based on the current docking simulations, it is suggested that these complexes may further be investigated for their inhibitory potential against the HI. These may serve as a surrogate for discovery of novel HI inhibitors.

Supplementary Materials: The following supporting information can be downloaded at: <https://www.mdpi.com/article/10.3390/molecules27134231/s1>, Figures S1–S12: 1H and 13C NMR spectra of compounds **1a**, **1b**, **1c**, **2a**, **2b** and **2c**.

Author Contributions: Conceptualization, A.N.; methodology, A.N. and S.Q.; X-ray analysis, A.N.; formal analysis, A.N. and S.Q.; molecular docking, F.J. and A.U.R.; writing—original draft preparation, A.N. and S.Q.; writing—review and editing, A.N., S.Q., F.J. and A.U.R.; supervision, A.N.; project administration, A.N.; funding acquisition, A.N. All authors have read and agreed to the published version of the manuscript.

Funding: This work was supported through the Annual Funding track by the Deanship of Scientific Research, Vice Presidency for Graduate Studies and Scientific Research, King Faisal University, Saudi Arabia (project no. AN000479).

Institutional Review Board Statement: Not applicable.

Informed Consent Statement: Not applicable.

Data Availability Statement: Supplementary crystallographic data can be obtained online free of charge via <http://www.ccdc.cam.ac.uk/conts/retrieving.html> (accessed on 17 June 2022) (or from the Cambridge Crystallographic Data Centre, 12 Union Road, Cambridge CB2 1EZ, UK; Fax: +44-1223-336-033; e-mail: deposit@ccdc.cam.ac.uk), deposition numbers CCDC-2161943 (L), CCDC-2161944 (1a), CCDC-2161948 (1b), CCDC-2161945 (1c), CCDC-2161946 (2a), and 2161947 (2c).

Acknowledgments: This work was supported through the Annual Funding track by the Deanship of Scientific Research, Vice Presidency for Graduate Studies and Scientific Research, King Faisal University, Saudi Arabia (Project No. AN000479). Alexander Goller from the chair of Inorganic Chemistry II, University of Bayreuth, is thanked for refining the single-crystal analysis data.

Conflicts of Interest: The authors declare no conflict of interest.

Sample Availability: Samples of the compounds 1a, 1b, 1c, 2a, 2b and 2c are available from the authors.

References

1. Khan, E.; Khan, S.; Gul, Z.; Muhammad, M. Medicinal Importance, Coordination Chemistry with Selected Metals (Cu, Ag, Au) and Chemosensing of Thiourea Derivatives. *Review. Crit. Rev. Anal Chem.* **2020**, *51*, 812–835. [[CrossRef](#)] [[PubMed](#)]
2. Steppeler, F.; Iwan, D.; Wojaczyńska, E.; Wojaczyński, J. Chiral Thioureas—Preparation and Significance in Asymmetric Synthesis and Medicinal Chemistry. *Molecules* **2020**, *25*, 401. [[CrossRef](#)] [[PubMed](#)]
3. Zhang, Z.; Schreiner, P.R. (Thio)urea organocatalysis—What can be learnt from anion recognition? *Chem. Soc. Rev.* **2009**, *38*, 1187–1198. [[CrossRef](#)] [[PubMed](#)]
4. Bregović, V.B.; Basarić, N.; Mlinarić-Majerski, K. Anion binding with urea and thiourea derivatives. *Coord. Chem. Rev.* **2015**, *29*, 80–124. [[CrossRef](#)]
5. Henderson, W.; Nicholson, B.K. Synthesis and electrospray mass spectrometry of platinum(II) complexes derived from thiourea dianions and the X-ray structure of [Pt{NMeC(=NCN)S}(COD)] (COD = CYCLO-OCTA-1,5-DIENE). *Polyhedron* **1996**, *15*, 4015–4024. [[CrossRef](#)]
6. Henderson, W.; Kemmitt, R.D.W.; Mason, S.; Moore, M.R.; Fawcett, J.; Russell, D.R. Thiadiazatrimethylenemethane and *N,N',P*-triphenylphosphonothioic diamide complexes of platinum(II). *J. Chem. Soc. Dalton Trans.* **1992**, *1*, 59–66. [[CrossRef](#)]
7. Pilato, R.S.; Eriksen, K.A.; Stiefel, E.I.; Rheingold, A.L. Generation of Cp₂Mo:S and cycloaddition of the molybdenum sulfido bond with di-*p*-tolylcarbodiimide. *Inorg. Chem.* **1993**, *32*, 3799–3800. [[CrossRef](#)]
8. Barman, M.K.; Sinha, A.K.; Nembenna, S. An Efficient and Recyclable Thiourea-Supported Copper(I) Chloride Catalyst for Azide–Alkyne Cycloaddition Reactions. *Green Chem.* **2016**, *18*, 2534–2541. [[CrossRef](#)]
9. Yang, D.; Chen, Y.-C.; Zhu, N.-Y. Sterically Bulky Thioureas as Air- and Moisture-Stable Ligands for Pd-Catalyzed Heck Reactions of Aryl Halides. *Org. Lett.* **2004**, *6*, 1577–1580. [[CrossRef](#)]
10. Dai, M.; Liang, B.; Wang, C.; Chen, J.; Yang, Z. Synthesis of a Novel C₂-Symmetric Thiourea and Its Application in the Pd-Catalyzed Cross-Coupling Reactions with Arenediazonium Salts under Aerobic Conditions. *Org. Lett.* **2004**, *6*, 221–224. [[CrossRef](#)]
11. Jia, D.-X.; Zhu, A.-M.; Deng, J.; Zhang, Y. New Complexes with a Sterically Hindered Thiourea: Syntheses and Crystal Structures of [Co(dchtu)₂Cl₂], [Zn(dchtu)₂(NCS)₂] and [Pb(dchtu)₆](SCN)₂·2C₂H₅OH (dchtu = *N,N'*-dicyclohexylthiourea). *Z. Anorg. Allg. Chem.* **2007**, *633*, 2059–2063. [[CrossRef](#)]
12. Shen, X.; Shi, X.; Kang, B.; Liu, Y.; Tong, Y.; Jiang, H.; Chen, K. Syntheses, crystal structures and properties of Zn(II) and Cd(II) complexes derived from *N*-(*o*-nitrophenyl)-*N'*-(methoxycarbonyl) thiourea(H₂omt) and 2,2'-bipyridine(bpy) or *o*-phenanthroline(phen). *Polyhedron* **1998**, *17*, 4049–4058. [[CrossRef](#)]
13. Moloto, M.J.; Malik, M.A.; O'Brien, P.; Motevalli, M.; Kolawole, G.A. Synthesis and characterisation of some *N*-alkyl/aryl and *N,N'*-dialkyl/aryl thiourea cadmium(II) complexes: The single crystal X-ray structures of [CdCl₂(CS(NH₂)NHCH₃)₂]_n and [CdCl₂(CS(NH₂)NHCH₂CH₃)₂]. *Polyhedron* **2003**, *22*, 595–603. [[CrossRef](#)]
14. Stocker, F.B.; Troester, M.A.; Britton, D. Crystal Structures of a Family of New Copper(I) Cyanide Complexes of Thiourea and Substituted Thioureas. *Inorg. Chem.* **1996**, *35*, 3145–3153. [[CrossRef](#)]
15. Stocker, F.B.; Britton, D.; Young, V.G., Jr. Crystal Structures of a Family of Silver Cyanide Complexes of Thiourea and Substituted Thioureas. *Inorg. Chem.* **2000**, *39*, 3479–3484. [[CrossRef](#)]

16. Leßmann, F.; Beyer, L.; Sieler, J. Synthesis and X-ray structure of the first chloro-bridged thiourea mercury(II) complex $[C_6H_5C(OCH_3)NC(S)N(C_2H_5)_2HgCl_2]_2$. *Inorg. Chem. Commun.* **2000**, *3*, 62–64. [[CrossRef](#)]
17. Bierbach, U.; Hambley, T.W.; Farrell, N. Modification of Platinum(II) Antitumor Complexes with Sulfur Ligands. 1. Synthesis, Structure, and Spectroscopic Properties of Cationic Complexes of the Types $[PtCl(diamine)(L)]NO_3$ and $[PtCl(diamine)]_2(L-L)(NO_3)_2$ (L = Monofunctional Thiourea Derivative; L-L = Bifunctional Thiourea Derivative). *Inorg. Chem.* **1998**, *37*, 708–716.
18. Bowmaker, G.A.; Pakawatchai, C.; Saitong, S.; Skelton, B.W.; White, A.H. Structural and spectroscopic studies of some adducts of silver(I) halides with thiourea and N-ethyl substituted thioureas. *Dalton Trans.* **2010**, *39*, 4391–4404. [[CrossRef](#)]
19. Bowmaker, G.A.; Hanna, J.V.; Pakawatchai, C.; Skelton, B.W.; Thanyasirikul, Y.; White, A.H. Crystal Structures and Vibrational Spectroscopy of Copper(I) Thiourea Complexes. *Inorg. Chem.* **2009**, *48*, 350–368. [[CrossRef](#)]
20. Bowmaker, G.A.; Chaichit, N.; Hanna, J.V.; Pakawatchai, C.; Skelton, B.W.; White, A.H. Spectroscopy and structures of two complete families, one mononuclear, the other binuclear, of 1:2 CuX:dptu stoichiometry (X = Cl, Br, I; 'dptu' = N,N'-diphenylthiourea). *Dalton Trans.* **2009**, 8308–8316. [[CrossRef](#)]
21. Ramadas, K.; Janarthanan, N.; Velmathi, S. Lac Sulfur Assisted Synthesis of Symmetrical Thioureas. *Synth. Commun.* **1997**, *27*, 2255–2260. [[CrossRef](#)]
22. Chetana, P.; Srinatha, B.; Somashekar, M.; Policegoudra, R. Synthesis, spectroscopic characterisation, thermal analysis, DNA interaction and antibacterial activity of copper(I) complexes with N, N'-disubstituted thiourea. *J. Mol. Struct.* **2016**, *1106*, 352–365. [[CrossRef](#)]
23. Mahendiran, D.; Amuthakala, S.; Bhuvanesh, N.S.P.; Kumar, R.S.; Rahiman, A.K. Copper complexes as prospective anticancer agents: In vitro and in vivo evaluation, selective targeting of cancer cells by DNA damage and S phase arrest. *RSC Adv.* **2018**, *8*, 16973–16990. [[CrossRef](#)]
24. Canudo-Barreras, G.; Ortego, L.; Izaga, A.; Marzo, I.; Herrera, R.P.; Gimeno, M.C. Synthesis of New Thiourea-Metal Complexes with Promising Anticancer Properties. *Molecules* **2021**, *26*, 6891. [[CrossRef](#)]
25. Yan, K.; Lok, C.-N.; Bierla, K.; Che, C.-M. Gold(I) complex of N,N'-disubstituted cyclic thiourea with in vitro and in vivo anticancer properties—Potent tight-binding inhibition of thioredoxin reductase. *Chem. Commun.* **2010**, *46*, 7691–7693. [[CrossRef](#)]
26. Rehm, T.; Rothmund, M.; Muenzner, J.K.; Noor, A.; Kempe, R.; Schobert, R. Novel cis- $[(NHC)_1(NHC)_2(L)Cl]$ platinum(ii) complexes—Synthesis, structures, and anticancer activities. *Dalton Trans.* **2016**, *45*, 15390–15398. [[CrossRef](#)]
27. Muenzner, J.K.; Rehm, T.; Biersack, B.; Casini, A.; de Graaf, I.; Worawutputtpong, P.; Noor, A.; Kempe, R.; Brabec, V.; Kasparkova, J.; et al. Adjusting the DNA Interaction and Anticancer Activity of Pt(II) N-Heterocyclic Carbene Complexes by Steric Shielding of the Trans Leaving Group. *J. Med. Chem.* **2015**, *58*, 6283–6292. [[CrossRef](#)]
28. Shahzad, A.; Khan, E.; Said, M.; Khan, G.S.; Syed, M.G.; Noor, A.; Zahoor, M.; Ullah, R.; Bari, A. Complexes of 1,3-Diisobutyl Thiourea with Copper(I), Zinc(II) and Mercury(II): Their Antioxidant and Antibacterial Evaluation. *Crystals* **2021**, *11*, 989. [[CrossRef](#)]
29. Khan, I.N.V.; Ali, Z.; Ibrahim, M.; Shujah, S.; Ali, S.; Ikram, M.; Rehman, S.; Khan, G.S.; Wadood, A.; Noor, A.; et al. Synthesis, characterization, antioxidant, antileishmanial, anticancer, DNA and theoretical SARS-CoV-2 interaction studies of copper(II) carboxylate complexes. *J. Mol. Struct.* **2022**, *1253*, 132308.
30. Naz, S.; Zahoor, M.; Umar, M.; Alghamdi, S.; Sahibzada, M.U.K.; UlBari, W. Synthesis, characterization, and pharmacological evaluation of thiourea derivatives. *Open Chem.* **2020**, *18*, 764–777. [[CrossRef](#)]
31. Faidallah, H.M.; Al-Mohammadi, M.M.; Alamry, K.A.; Khan, K.A. Synthesis and biological evaluation of fluoropyrazolesulfonylurea and thiourea derivatives as possible antidiabetic agents. *J. Enzyme Inhib. Med. Chem.* **2016**, *31*, 157–163. [[CrossRef](#)] [[PubMed](#)]
32. Rehman, T.U.; Khan, I.U.; Riaz, S. Novel substituted 3-phenyl 1-(4-(5-bromopyridin-3-yl)-6-phenylpyrimidin-2-yl)-thiourea compounds as key small organic molecules for the potential treatment of type II diabetes mellitus: In vitro studies against yeast α -glucosidase. *Med. Chem. Res.* **2017**, *26*, 1098–1106. [[CrossRef](#)]
33. Noor, A.; Qayyum, S.; Jabeen, F. Selective synthesis of mono(amidinate) chromium(II) chloride complexes and a computational insight of their interaction with human insulin. *Polyhedron* **2021**, *194*, 114942. [[CrossRef](#)]
34. Findlater, M.; Hill, N.J.; Cowley, A.H. Synthesis and structure of two new (guanidinate)boron dichlorides and their attempted conversion to boron(i) derivatives. *Dalton Trans.* **2008**, *33*, 4419–4423. [[CrossRef](#)]
35. Altomare, A.; Burla, M.C.; Camalli, M.; Cascarano, G.L.; Giacovazzo, C.; Guagliardi, A.; Moliterni, A.G.G.; Polidori, G.; Spagna, R. SIR 97: A new tool for crystal determination and refinement. *J. Appl. Cryst.* **1999**, *32*, 115–119. [[CrossRef](#)]
36. Sheldrick, G.M. Crystal structure refinement with SHELXL. *Acta Cryst.* **2015**, *C71*, 3–8.
37. Farrugia, L.J. WinGX suite for small-molecule single-crystal crystallography. *J. Appl. Cryst.* **1999**, *32*, 837–838. [[CrossRef](#)]
38. Dolomanov, O.V.; Bourhis, L.J.; Gildea, R.J.; Howard, J.A.K.; Puschmann, H. OLEX2: A Complete Structure Solution, Refinement and Analysis Program. *J. Appl. Cryst.* **2009**, *42*, 339–341. [[CrossRef](#)]
39. Molecular Operating Environment (MOE), 2020.09 Chemical Computing Group ULC, 1010 Sherbooke St. West, Suite #910, Montreal, QC, Canada, H3A 2R7, 2020. Available online: <https://www.chemcomp.com> (accessed on 27 February 2022).
40. Chinai, J.M.; Taylor, A.B.; Ryno, L.M.; Hargreaves, N.D.; Morris, C.A.; Hart, P.J.; Urbach, A.R. Molecular recognition of insulin by a synthetic receptor. *J. Am. Chem. Soc.* **2011**, *133*, 8810–8813. [[CrossRef](#)]
41. Rodrigues, C.H.; Pires, D.E.; Ascher, D.B. DynaMut: Predicting the impact of mutations on protein conformation, flexibility and stability. *Nucleic Acids Res.* **2018**, *46*, W350–W355. [[CrossRef](#)]

42. Hollup, S.M.; Salensminde, G.; Reuter, N. WEBnm@: A web application for normal mode analyses of proteins. *BMC Bioinform.* **2005**, *6*, 52. [[CrossRef](#)]
43. Soriano-Garcia, M.; Chavez, G.T.; Cedillo, F.D.; Perez, A.E.D.; Hernandez, G.A. Crystal Structures of *N,N'*-(*m*-Tolyl)thiourea and *N'*-(*p*-Tolyl)thiourea. *Anal. Sci.* **2003**, *19*, 1087–1088. [[CrossRef](#)]
44. Shahwar, D.; Tahir, M.N.; Khan, M.A.; Ahmad, N.; Furqan, M. 1,3-Bis(3-methylphenyl)thiourea: Triclinic polymorph. *Acta Crystallogr. Sect. E Struct. Rep. Online* **2009**, *E65*, o482. [[CrossRef](#)]
45. Qin, Y.-Q.; Jian, F.-F.; Liang, T.-L. 1,3-Bis(4-chlorophenyl)thiourea. *Acta Crystallogr. Sect. E Struct. Rep. Online* **2006**, *E62*, o5043–o5044. [[CrossRef](#)]
46. Sarojini, B.K.; Narayana, B.; Swamy, M.T.; Yathirajan, H.S.; Bolte, M. Redetermination of *N,N'*-bis(4-chlorophenyl)thiourea at 173 K. *Acta Crystallogr. Sect. E Struct. Rep. Online* **2007**, *E63*, o3879. [[CrossRef](#)]
47. Csonka-Horvai, J.; David, A.; Horvath, G.; Naray-Szabo, G. Rotational Isomerism in Bis-[*p*-(3-Methyl-butyloxy)-phenyl]-thiourea. *Z. Naturforsch. B* **1971**, *26*, 21–23. [[CrossRef](#)]
48. Kotke, M.; Schreiner, P.R. Acid-free, organocatalytic acetalization. *Tetrahedron* **2006**, *62*, 434–439. [[CrossRef](#)]
49. Soriano-Garcia, M.; Chavez, G.T.; Dominguez Perez, A.E.; Hernandez, G.A. Crystal Structure of *N*-2-Tolyl-*N'*-4-tolyl-thiourea. *Anal. Sci.* **2001**, *17*, 907–908. [[CrossRef](#)]
50. Muhammed, N.; Rahman, Z.-U.; Ali, S.; Meetsma, A. 1,3-Bis(4-bromophenyl)thiourea. *Acta Crystallogr. Sect. E Struct. Rep. Online* **2007**, *E63*, o632–o633. [[CrossRef](#)]
51. Muhammed, N.; Rahman, Z.-U.; Ali, S.; Meetsma, A. 1,3-Di-*o*-tolylthiourea. *Acta Crystallogr. Sect. E Struct. Rep. Online* **2007**, *E63*, o634–o6353. [[CrossRef](#)]
52. Kuan, F.S.; Tiekink, E.R.T. *N,N'*-Di-*o*-tolylthiourea. *Acta Crystallogr. Sect. E Struct. Rep. Online* **2007**, *E63*, o4692. [[CrossRef](#)]
53. Ramnathan, A.; Sivakumar, K.; Subramanian, K. Symmetrically substituted thiourea derivatives. *Acta Crystallogr. Sect. C Cryst. Struct. Commun.* **1995**, *C51*, 2446–2450. [[CrossRef](#)]
54. Srivastava, P.C.; Dwivedi, S.; Singh, V.; Butcher, R.J. Mono- and bis(dialkyl/aryl dithiocarbamate) complexes of 1,1,2,3,4,5,6-heptahydro-1,1-dihalido telluranes: Synthesis, spectroscopy, structures and cleavage reaction. *Polyhedron* **2010**, *29*, 2202–2212. [[CrossRef](#)]
55. Ramnathan, A.; Sivakumar, K.; Subramanian, K.; Janarthanan, N.; Ramadas, K.; Fun, H.-K. 1,3-Bis(3-chlorophenyl)thiourea. *Acta Crystallogr. Sect. C Cryst. Struct. Commun.* **1996**, *C52*, 134–136. [[CrossRef](#)]
56. Štrukil, V.; Igrc, M.D.; Fábíán, L.; Eckert-Maksić, M.; Childs, S.L.; Reid, D.G.; Duer, M.J.; Halasz, I.; Mottillo, C.; Friščić, T. A model for a solvent-free synthetic organic research laboratory: Click-mechanosynthesis and structural characterization of thioureas without bulk solvents. *Green Chem.* **2012**, *14*, 2462–2473. [[CrossRef](#)]
57. Allen, F.H.; Kennard, O.; Watson, D.G.; Brammer, L.; Orpen, A.G.; Taylor, R. Tables of bond lengths determined by X-ray and neutron diffraction. Part 1. Bond lengths in organic compounds. *J. Chem. Soc. Perkin Trans.* **1987**, *2*, S1–S19. [[CrossRef](#)]
58. Yuan, Y.-F.; Ye, S.-M.; Zhang, L.-Y.; Wang, B.; Xu, Y.-M.; Wang, J.-T.; Wang, H.-G. Studies on intramolecular hydrogen bonding of 1,1'-bis[*N*-formyl-*N'*-*p*-chlorophenylthiourea]ferrocene. *Inorg. Chim. Acta* **1997**, *256*, 313–318. [[CrossRef](#)]
59. Yuan, Y.-F.; Ye, S.-M.; Zhang, L.-Y.; Wang, J.-T. Coordination compounds derived from 1,1'-bis(*N*-formyl-*N'*-substituted thiourea)ferrocene derivatives and copper chloride; crystal structure of the copper chloride 1,1'-bis(*N*-formyl-*N'*-isopropylthiourea)ferrocene coordination polymer. *Transition Met. Chem.* **1997**, *22*, 561–564. [[CrossRef](#)]
60. Mufakkar, M.; Tahir, M.N.; Ahmad, S.; Shaheen, M.A.; Waheed, A. Bromidobis(*N,N'*-diphenylthiourea-κS)-copper(I) monohydrate. *Acta Cryst.* **2009**, *E65*, m892–m893.
61. Jia, D.; Zhu, A.; Ji, M.; Zhang, Y. Copper(I) halide complexes with a sterically hindered thiourea: Synthesis and crystal structures of [Cu(dctu)₂Cl] and [Cu(dctu)₂Br] (dctu = *N,N'*-dicyclohexylthiourea). *J. Coord. Chem.* **2008**, *61*, 2307–2314. [[CrossRef](#)]
62. Mufakkar, M.; Ahmad, S.; Khan, I.U.; Fun, H.-K.; Chantrapromma, S. Tetrakis(*N*-methylthiourea-κS)copper(I) iodide. *Acta Cryst.* **2007**, *E63*, m2384.
63. Khan, I.U.; Mufakkar, M.; Ahmad, S.; Fun, H.-K.; Chantrapromma, S. Tris(*N,N'*-dibutylthiourea-κS)iodidocopper(I) 0.6-hydrate. *Acta Cryst.* **2007**, *E63*, m2550–m2551. [[CrossRef](#)]
64. Ahmad, S.; Mufakkar, M.; Khan, I.U.; Fun, H.-K.; Waheed, A. Hexakis(μ₃-1-methylthiourea-κ₃S:S:S)-hexakis[iodidocopper(I)]. *Acta Cryst.* **2012**, *E68*, m1405–m1406.
65. Rahmani, F.R.; Malik, A.U.; Ahmad, N. Studies on mixed ligand complexes of Ag(I)—II. Interaction of silver halides with substituted thiourea and heterocyclic amines. *J. Inorg. Nucl. Chem.* **1977**, *39*, 2089–2092. [[CrossRef](#)]
66. Rahmani, F.R.; Malik, A.U.; Ahmad, N. Studies on mixed ligand complexes of silver(I) halides—I. Interaction of silver(I) thiourea, naphthyl and diphenyl thiourea halides with pyridine, 2,2'-dipyridyl and 1,10-phenanthroline. *J. Inorg. Nucl. Chem.* **1976**, *38*, 2119–2121. [[CrossRef](#)]
67. Aulakh, J.K.; Lobana, T.S.; Sood, H.; Arora, D.S.; Garcia-Santos, I.; Kaur, M.; Jasinski, J.P. Synthesis, structures, and novel antimicrobial activity of silver(I) halide complexes of imidazolidine-2-thiones. *Polyhedron* **2020**, *175*, 114235. [[CrossRef](#)]
68. Caballero, A.B.; Salas, J.M.; Moreno, M.S. Metal-Based Therapeutics for Leishmaniasis: A chapter I. In *Leishmaniasis-Trends in Epidemiology, Diagnosis and Treatment*; Claborn, D.M., Ed.; IntechOpen: London, UK, 2014.